Exp. Theo. NANOTECHNOLOGY 9 (2025) 373-384 https://doi.org/10.56053/9.S.373

Enhancing the anticorrosion of graphene/epoxy nanocomposites with ZrO_2 nanoparticles

Estabraq Talib Abdullah[1,*], *Malik Rashid Khasheet*[1], *Zainab Naseer Hasheem*[2]

[1]Physics Department, College of Science, University of Baghdad, Baghdad, Iraq
[2]Department of Radiology Techniques, College of Health & Medical Techniques, Al-Esraa University, Baghdad, Iraq
[*]) Email: estabraqtalib@sc.uobaghdad.edu.iq

Received 11/2/2025, *Received in revised form* 12/3/2025, *Accepted* 19/3/2025, *Published* 15/5/2025

The corrosion of metallic equipment and the degradation of plastic materials pose significant concerns for companies and national economies. These issues must be addressed by researching and implementing creative procedures and techniques. A practical solution can be found by developing materials that can withstand corrosive conditions and can be applied as protective coatings to hinder or, at the very least, slow down the degradation process. This work synthesized and applied nanocomposite coatings of graphene/zirconia dioxide (ZrO_2)/epoxy to protect oil pipelines from corrosion. The graphene/ ZrO_2/epoxy hybrid is synthesized using mechanical stirring and ultrasonication. The main characteristics are confirmed by scanning electron microscopy (SEM), Fourier-transform infrared spectroscopy (FTIR), and absorbance analysis. The ability of graphene/ZrO_2 to protect epoxy from corrosion is studied at temperatures ranging from 298 to 318 K. The effectiveness of these coatings in preventing corrosion on the surface is investigated by measuring the corrosion potential (ECorr) and the corrosion current (ICorr) using a potentiostat. Investigations revealed that the corrosion protective properties are significantly enhanced by adding graphene/ZrO_2 to epoxy. The enhancement is attributed to the sheet-like structure, uniform dispersion, and graphene/ ZrO_2 hybrid exfoliation within the epoxy matrix, which effectively prevents the underlying metal substrate from being corroded.

Keywords: Epoxy; AFM; ZrO_2; SEM; Graphene.

1. INTRODUCTION

Corrosion, the deterioration of metals through chemical interaction with their surrounding environment, is a growing concern. This phenomenon has the potential to significantly harm society and industry globally [1, 2]. In recent decades, numerous methods for the protection of metal substrates have garnered significant attention to resolve this issue, including cathodic protection, anodic protection, corrosion inhibitors, coating, and alloying [3, 4]. Polymer coatings are the most effective method of preventing metals from corrosion among the numerous approaches. The anti-corrosion properties, chemical stability, minimal shrinkage, excellent adhesion, thermal stability, and electrical resistance of epoxy resins, which are similar to a conventional coating, make them widely used as polymeric coatings, composite matrices, adhesives, and structural materials [5, 6]. Regrettably, epoxy also possesses some undesirable characteristics, including brittleness, poor flexibility, and impact resistance [7]. This results in the rapid production of a large number of small apertures during the fabrication of high-temperature-curing epoxy solvent-borne coatings, which may compromise their barrier properties. Consequently, numerous researchers are inclined to fortify epoxy by incorporating thermoplastics, rubbers, or nanofillers [8, 9]. The high specific surface area, small size, functionality, and cost-effective preparation of nanoparticles in epoxy make them a common method for providing durable protection for substrates, among various toughening methods [10, 11].

The safe operation of oil and gas pipelines is concerned with corrosion in oil and gas production operations. Multi-phase flow corrosion media in which characterize the corrosion CO_2, H_2S, and acidic materials coexist with oil, gas, and water. Water is the main corrosion medium CO_2, H_2S, and high Cl^- are more likely to cause localized corrosion. In addition, some pipelines experience higher temperatures. The rate of localized corrosion accelerates, leading to corrosion failure and exposing hidden hazards in the operation of pipelines. It is necessary to perform sampling. Analyze the failed pipelines and investigate the root cause. Take control measures to ensure the prevention of corrosion failure and safe operation [12]. Consequently, this investigation aims to assess the impact of incorporating graphene and ZrO_2 (with different concentrations) into epoxy adhesives as a supplement to high-performance coatings for oil and gas pipeline applications.

2. EXPERIMENTAL

2.1 Materials

Graphene sheets with a thickness of 608 nm and an average particle diameter of 15μm, without any modification, are purchased from Skyspring Nanomaterials Inc. (USA). Epoxy resin Sikadur 52 LP A is obtained from Sika Chemicals Inc., Bahrain, and used as the matrix for mixing with graphene. It is a solvent-free; low-viscosity injection liquid based on high-strength epoxy resins. The hardening material is from the same company, and under the name Sikadur 52 LP oxide, ZrO_2 is provided by Changsha Santech, with a thickness of 5-30 nm and an average particle diameter of 20 nm. The chosen oil pipe sample has a disk shape. Specimens are cut into 1.5 cm diameter and 0.5 cm thick pieces of mild steel (ASTM A106 API 5L GRADE B SEAMLESS PIPES 6" SCH40 6M AM66007). These samples are polished with sandpapers of different grades, including 600, 800, 1200, and 2000 grit. Then, the samples are ished with distilled water and ethanol and allowed to dry for further use, as shown in Figure 1.

Figure 1 Steel sample.

2.2 Preparation Process

Epoxy-based nanocomposites reinforced with 0.08 wt% of graphene are the most successful percentage for the work, depending on many preparation experiments, and different weight ratios of ZrO_2 (0.2, 1.2, 2.2, and 3.2 %) are fabricated using the following procedures. A desired graphene concentration is added to an ultrasonicated liquid epoxy and mixed for 1 hour. The solution is further processed through mechanical stirring and sonication for 3 hours to separate the nanofiller aggregation and achieve a good dispersion. Then, ZrO_2 is added to the composite. Finally, the hardener is added to the mixture at a ratio of 1:2 and then ultrasonicated for an additional 15 minutes. The resulting graphene/ ZrO_2-epoxy mixture samples are cast into discs with dimensions of 1.5 × 0.5 cm and cured at 70 °C for 1 hour. The samples are detonated as variables, as in Table 1.

Table 1 Materials used in current work.

Materials	Symbols
Graphene	B1
Epoxy	B2
ZrO_2	B3
0.01 nanocomposites	B4
0.02 nanocomposites	B5
0.03 nanocomposites	B6
0.04 nanocomposites	B7

2.3 Characterization

Using a Shimadzu 8400 Fourier transform infrared spectrophotometer, a homogenized powder of the synthesized materials and KBr is pelletized and analyzed for structural characteristics in the 4000-400 cm^{-1} frequency range. Scanning electron microscopy (SEM) and atomic force microscopy (AFM) (Digital Instruments Co., Nanoscope Ia) are used to study the morphologies of the samples. Following ASTM D7334, a contact angle test is conducted to understand the surface alteration caused by nanoparticle incorporation into the composite. The computer looked at the camera's photos to determine the angle at which the water droplet made contact with the surface. Shanghai Brilliance Instruments

Limited, China, developed an electrochemical workstation for measuring electrochemical impedance spectroscopy (EIS). A reference electrode, typically a saturated calomel electrode (SCE), a counter electrode, usually a platinum grid, and a working electrode, often an EP-coated steel coupon, are the traditional components of a three-electrode setup. An electrolyte solution of 3.5% NaCl is used for the measurements conducted at room temperature in a 500-ml electrolyte cell. An electrochemical workstation running at 10^{4}-10^{-1} Hz and an AC amplitude of 10 mV is used to repeat the EIS measurements regularly. Then, ZSimpWin is used to examine the EIS data. The polarization measurements are carried out at a scan rate of 1 mV.s^{-1}, from -0.5 to 0.5 mV. We created a robust open-circuit electrode for all tests by exposing the samples to a 3.5% NaCl aqueous solution for 1 hour. A technique called Tafel extrapolation is used to examine the polarization curve characteristics. We employed three replicates to ensure the repeatability of all electrochemical measurements.

3. RESULT AND DISCUSSION

3.1 Structural and morphological analysis

Figure 2a and b show the non-crystalline distribution of ZrO_2 and graphene within the epoxy matrix (B5 and B7). A homogeneous distribution of ZrO_2 particles is observed, along with a uniform distribution of graphene throughout the matrix. Additionally, nanoscale particles exhibited a homogeneous distribution across the sample, with no evidence of graphene and ZrO_2 clustering on the epoxy surface [1-3].

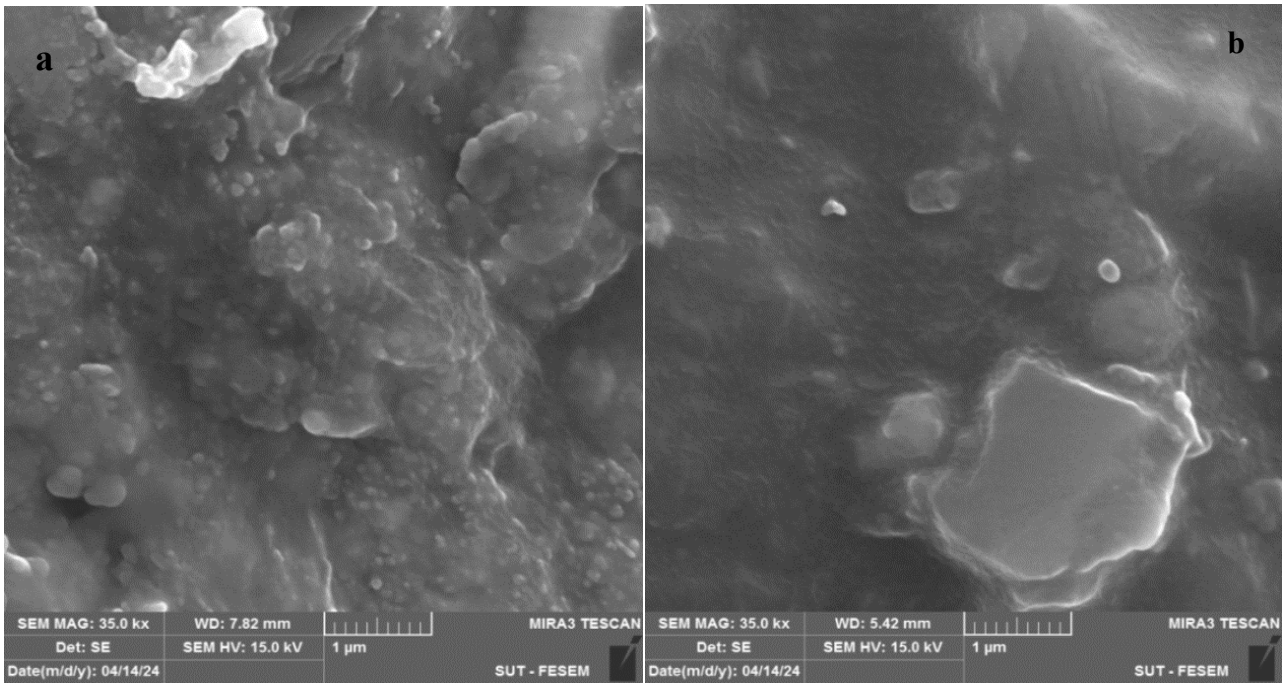

Figure 2 SEM images of (a) B5 and (b) B7 nanocomposites.

Figure 3 exhibits the FTIR spectra of pure graphene, ZrO_2, and epoxy. The spectra revealed distinct bands of bending and stretching vibrations associated with the functional groups generated in the synthesis. For epoxy, the peak at 3421.72 cm^{-1} corresponds to O-H stretching. Peaks at 2966 and 2925 cm^{-1} correspond to the -CH-O-CH2- stretching of the epoxy ring, and the asymmetric stretching of the -CH3- and -CH2- bonds are all recognized. The peak at 3050 cm^{-1} is also significant. Both data sets show symmetric stretching, with a peak at 2958.80 cm^{-1} corresponding to the C-H (alkanes) stretching. The benzene ring is usually related to the aromatic ring's C-H bond harmonics and signs of the stretching of C=C-H in the 2000 to 1500 cm^{-1} range. The peak at 1510.28 cm^{-1} indicates C=C stretching, whereas peaks at 956.69 cm^{-1} indicate binding between the epoxy rings -CH-O-CH2- groups. Hence, 1247.94 cm^{-1} represents the C-O stretching [4]. The stretching vibrations of the graphene's hydroxyl (O-H) and

carbonyl (C=C) groups are associated with two distinct peaks, one at 3747 cm^{-1} and the other at 1670 cm^{-1}. The OH group's ability to form strong hydrogen bonds with various surfaces and exhibit excellent stickiness makes it an integral component of graphene's structure. Its versatility makes it ideal for a wide range of uses, including material adhesion and adhesive installation [5, 6].

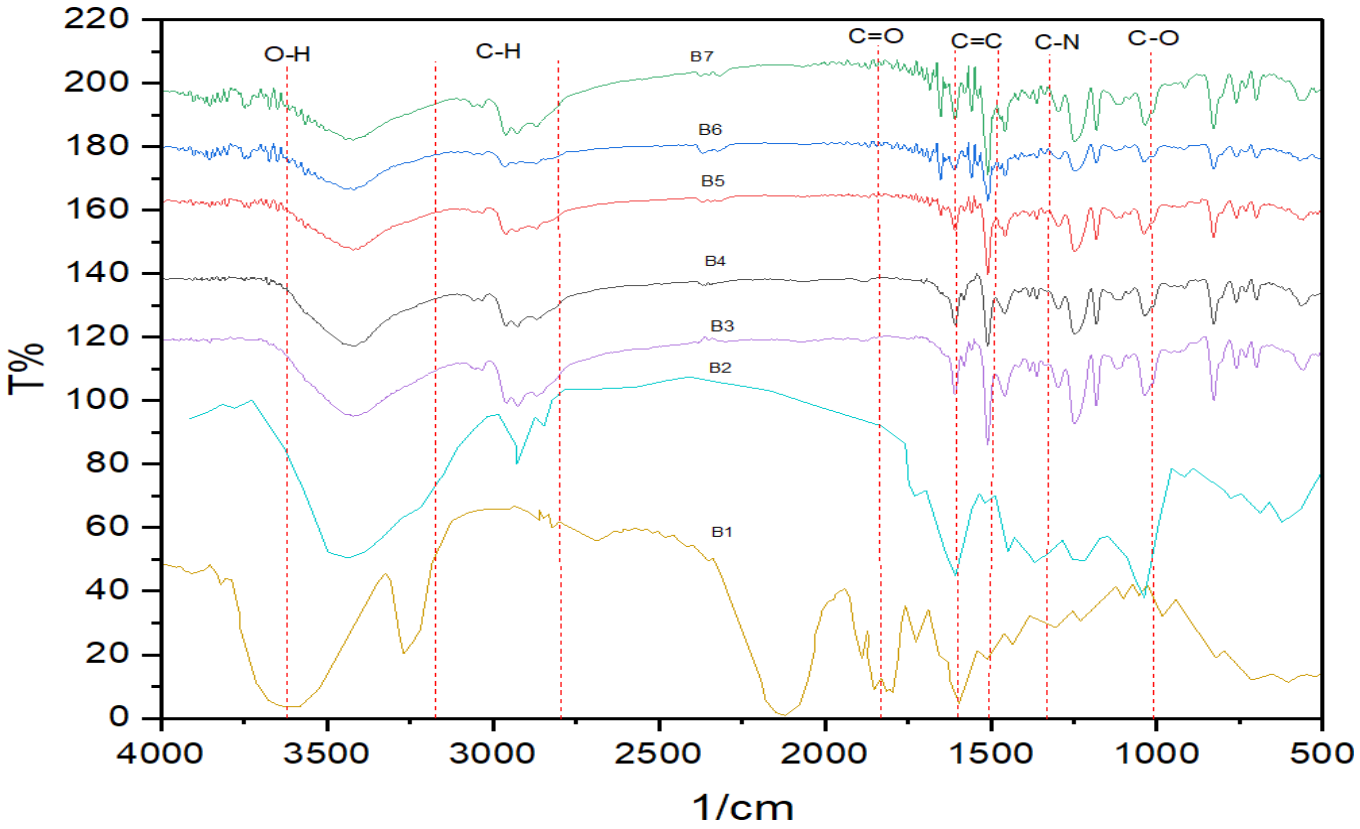

Figure 3 FTIR spectrum for pure graphene and nanocomposites.

The broad peak at 3418 cm^{-1} and the sharp peak at 1624 cm^{-1} represent the OH stretching and bending vibrations, respectively, for ZrO_2 nanoparticles. According to [7], the hydrated molecules could be in the hydroxyl group if the signal at 1430 cm^{-1} is any indication. The strong band represents the energetically neutral bonding states. The band at 680 cm^{-1} represents the Zr-O vibration in a tetragonal structure. The N-H bending introduced a new band at 1525 cm^{-1} to ZrO_2-epoxy graphene, and when the ZrO_2 concentration is raised, the peak at 1500 cm^{-1} grew, while the absorption peaks at 1670 cm^{-1} shrank. This point gives a degree of reaction between the epoxide and the amino group [8].

3.2 AFM analysis and surface roughness

Figure 4 show that the AFM revealed the homogeneity of the composite's coating layers (B2, B4, B5, B6, and B7). Adding graphene/ZrO_2 to epoxy in an uneven way (Table 2) decreased its average roughness (Sa). This suggests that using a hybrid material for reinforcement makes the process more uniform, leading to better protection properties. The findings revealed that incorporating a small amount of graphene-ZrO_2 reduced the surface roughness [9]. Figure 5 depicts the contact angle between the epoxy and the samples. The epoxy contact angle is about 67.98°, which showed that epoxy is hydrophilic [10]. Table 2 illustrates a clear trend in the contact angle of the nanocomposites with different amounts of graphene-ZrO_2. This is especially true for the 0.02 wt% nanocomposite.

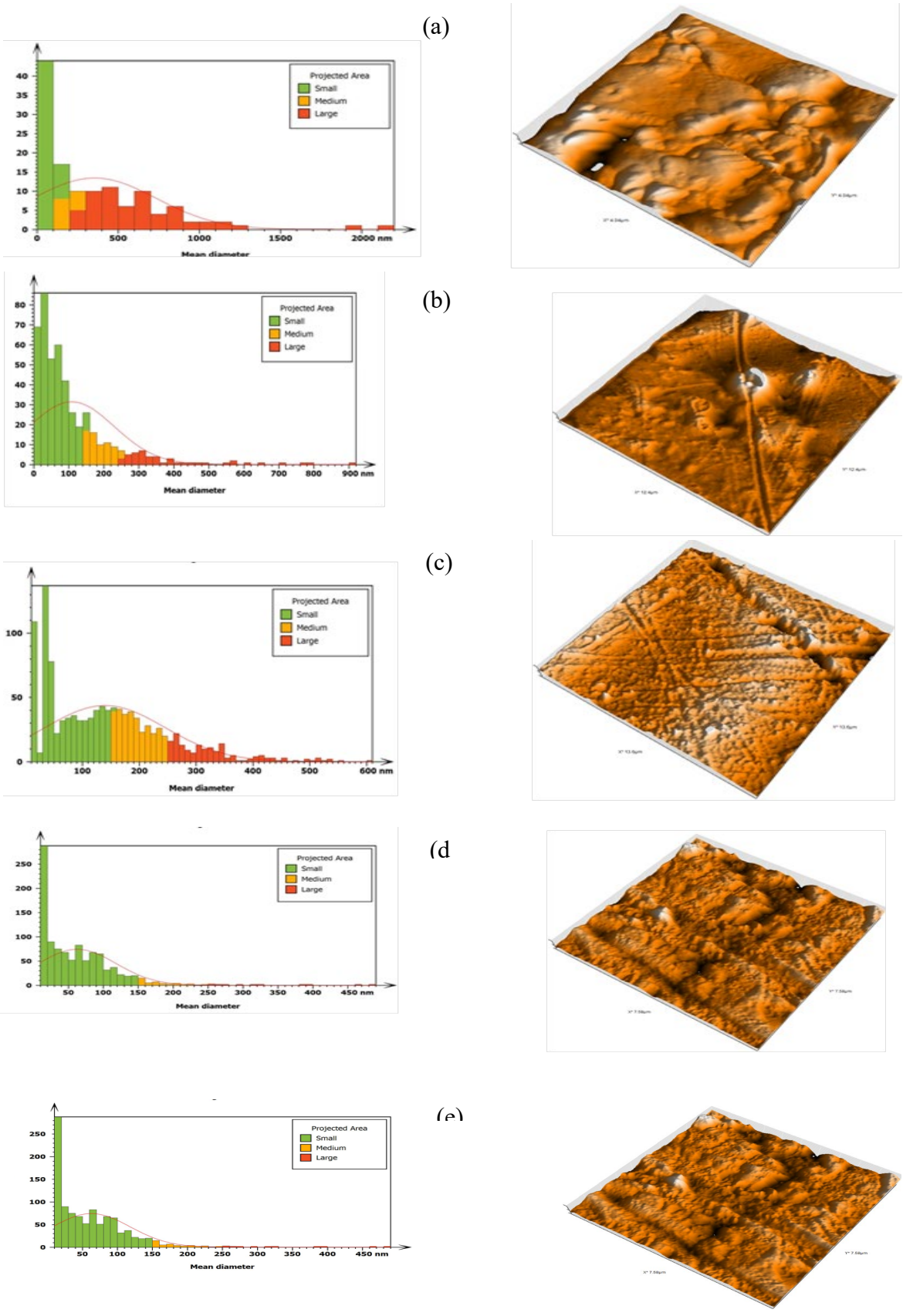

Figure 4 AFM images of (a) B2, (b) B4, (c) B5, (d) B6, and (e) B7.

Table 2 Surface roughness and contact angle of epoxy and nanocomposites.

Symbols	Contact angle	Sa (nm)
B2	67.98º	244.2
B4	58.78º	150.5
B5	91.45º	191.4
B6	80.46º	27.93
B7	81.27º	101.2

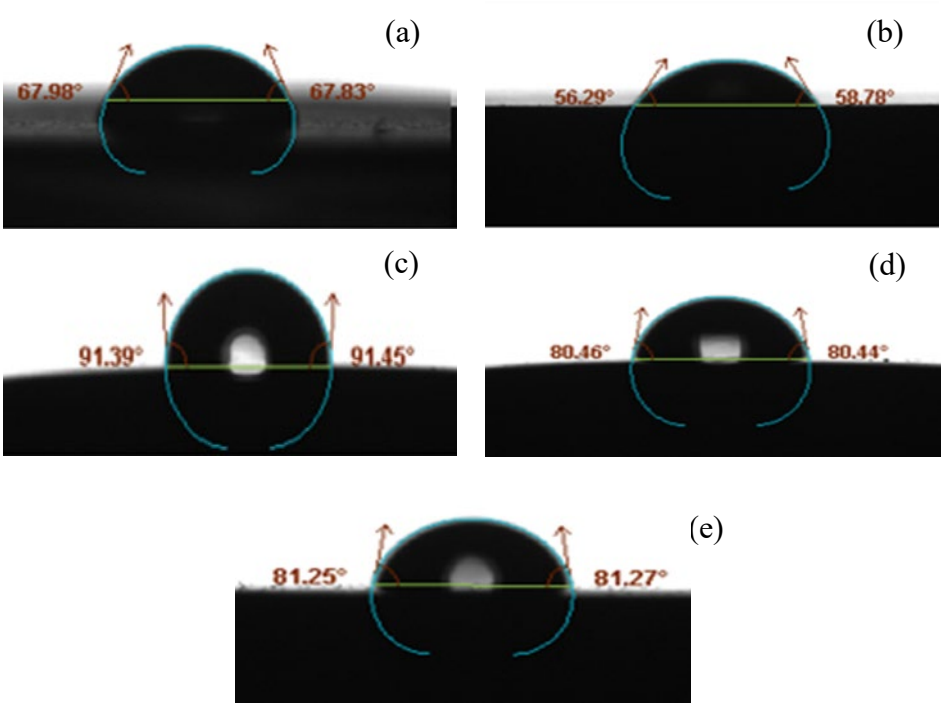

Figure 5 Contact angle of (a) B2, (b) B4, (c) B5, (d) B6, and (e) B7.

AFM confirmed the increased surface hydrophobicity of the graphene-ZrO_2 samples by measuring the surface, Sa, of the nanocomposites [10, 11]. The surface inside the frame of a compact fluid bead exhibited the highest elevated value of 91° at B5, as shown in Figure 5c. The presence of leftover oxygen groups on the coating's surface, along with the graphene and ZrO_2 structures, may explain this phenomenon. Coated surfaces may exhibit varying wetting abilities due to their chemical composition and/or surface roughness [12]. This outcome suggests a shift in the surface's chemical composition, roughness, and water capillary penetration (porosity). This can be attributed to the low hydrophilicity and barrier effect of the nanofillers in the nanocomposites. This leads to a decrease in the coated surface's penetration and significantly improved corrosion protection.

3.3 Absorption spectrum

The absorption test is used to determine the amount of fluid in the body after a specific period under specific conditions. Factors that affect liquid absorption include the material's composition, additives applied, temperature, pressure, and duration of exposure to heat, all of which affect the metal's final

properties. We collected rainwater with a pH of 6.8. The samples are selected based on the contact angle (B5, B7). The samples are immersed in rainwater in a cylindrical plastic container and left there for seven days. Next, the samples are immersed in crude oil with a salt concentration of 130 ppm for seven days. The samples are placed in a container containing the gasoline solution. Also, we recorded the weight daily for the next seven days using an empathetic scale and recorded variables to determine the amount absorbed, as shown in Table 3.

Table 3 The weight daily for samples immersed in solutions.

Time	Weight (g) before test of (0.02 %)	Weight after test(g)	Weight (g) before test of (0.04%)	Weight after test(g)
First day	5.60	5.60	5.85	5.85
Second day	5.60	5.60	5.85	5.85
Third day	5.60	5.60	5.85	5.85
Fourth day	5.60	5.60	5.85	5.85
Fifth day	5.60	5.60	5.85	5.85
Sixth day	5.60	5.60	5.85	5.85
Seventh day	5.60	5.60	5.85	5.85

3.4 Corrosion Analysis

EIS effectively characterizes the coatings' anticorrosive efficacy. Nyquist plot, Figure 6(a), obtained from EIS measurements for the two ratios (0.2 and 0.4 wt%) for two different temperatures (25 and 45 °C). The Nyquist plot showed a large semi-circle curve, which proves the high electrochemical impedance. The Figure, in good agreement, confirms the positive effects of adding graphene nanoparticles to the polymer. Graphene and ZrO_2 nanoparticles enhanced barrier performance of the nanocomposite's coatings', acting as an effective barrier for the substrate and potentially exhibiting good dispersion. This resulted in outstanding corrosion resistance [13]. The increase in temperature led to a decrease in the samples' corrosion resistance. The coating film at 0.4 wt% at 45 °C suggested providing an effective barrier for corrosion, while 0.2 wt% showed a lower contribution to corrosion, possibly due to the agglomeration of nanoparticles and graphene. Also, Figure 6(b) of the Tafel plots showed that the corrosion current density (icorr) value went down at a ratio of 0.4 wt% and a temperature of 45 °C, which means the corrosion rate went down. This is a strong indication that the sample offers superior corrosion resistance. In addition, the various parameters obtained from the Tafel plot supported the study of high corrosion protection through oxidation and reduction rates. We studied the kinetics of the anodic and cathodic reactions using polarization measurements. The OCP plots also showed a slight decrease in voltage over time; at 45 °C, 0.4 wt% is the least fluctuating and most stable ratio, indicating slower corrosion rates.

In Figure 6 (c), the voltage changes slightly and slowly, indicating that the sample is stable and does not exhibit rapid deterioration. The results of the various tests suggest that the sample exhibits excellent overall corrosion resistance.

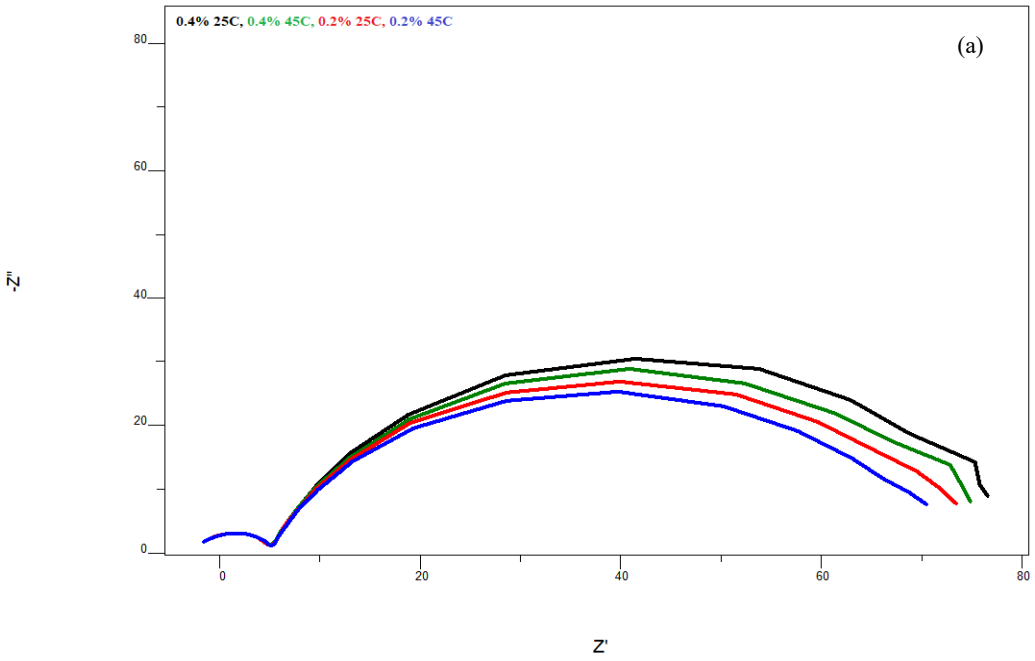
0.4% 25C, 0.4% 45C, 0.2% 25C, 0.2% 45C
(a)
-Z''
Z'
0
20
40
60
80

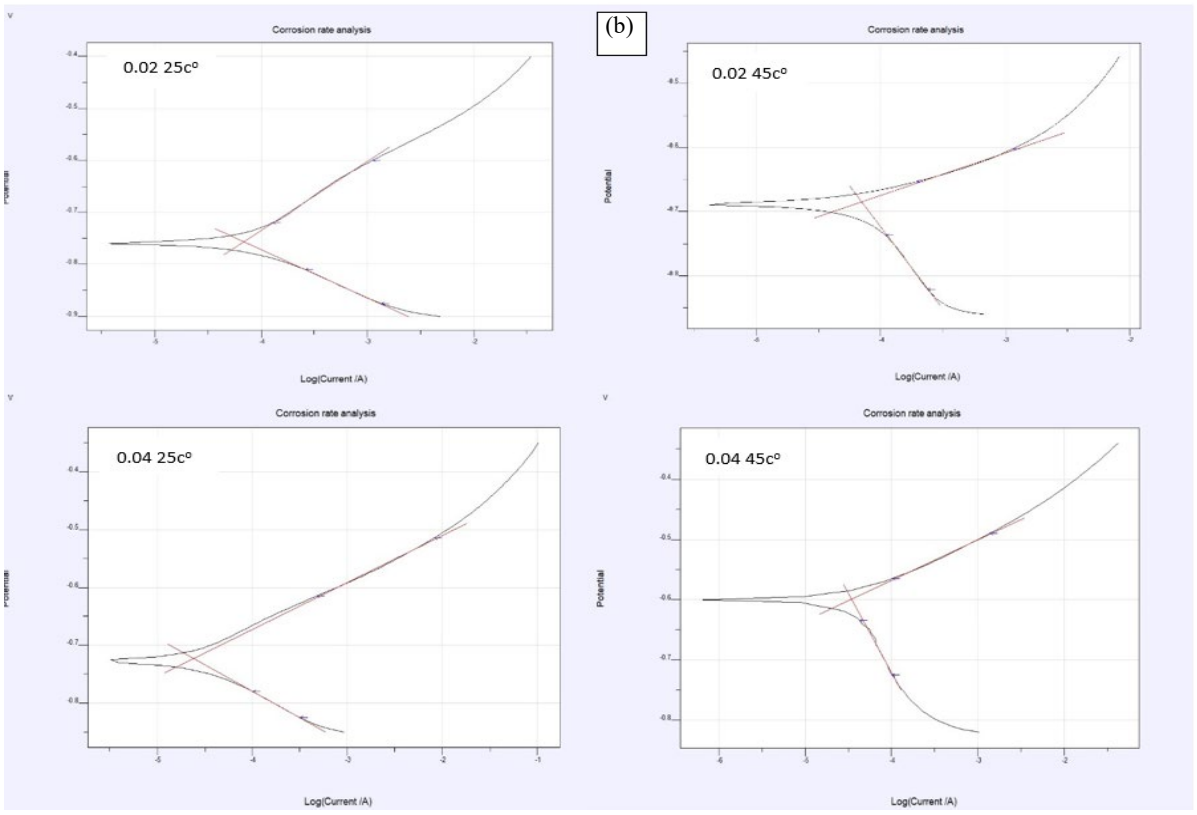
(b)
Corrosion rate analysis
0.02 25c°
0.02 45c°
0.04 25c°
0.04 45c°
Potential
Log(Current /A)

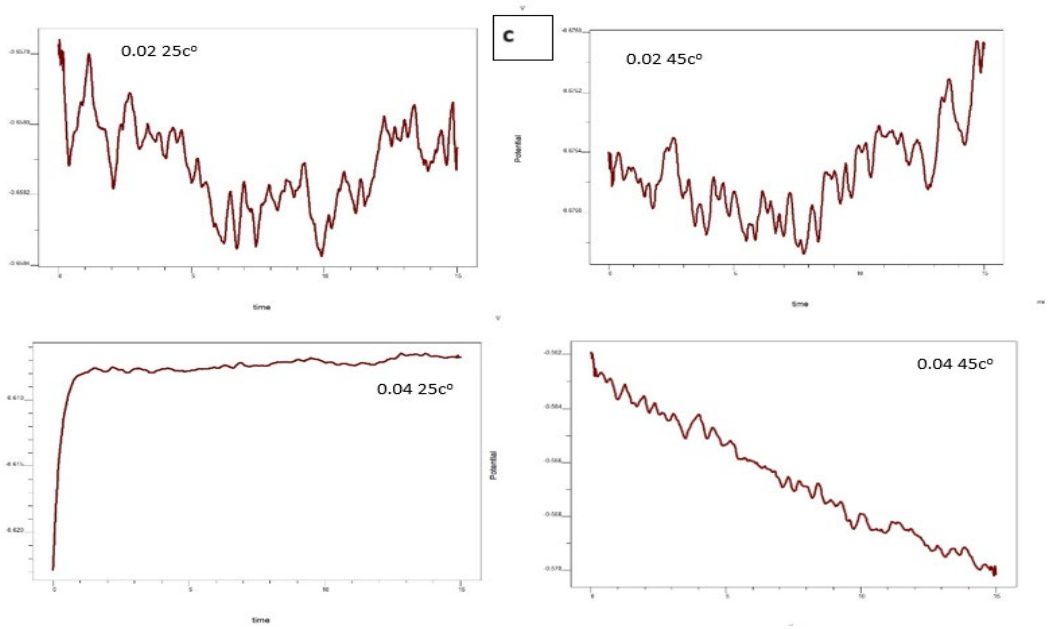

Figure 6 Corrosion tests (0. 2,0.4 wt%) (a) Eis test (b) Tafel test (c) Ocp test.

4. CONCLUSIONS

It was concluded that epoxy nanocomposite coatings filled with graphene and ZrO_2 exhibited a significant improvement in anti-corrosion performance compared to neat epoxy coating samples. The evenly distributed graphene/ZrO_2 in the epoxy matrix, consisting of two-dimensional sheets capable of filling tiny holes, exhibited a superior barrier effect, making the materials more resistant to corrosion. As a result, the newly prepared hybrid coatings may open up a new range of epoxy-containing sheet-like structures for corrosion protection.

ACKNOWLEDGMENTS

The authors express gratitude to their respective universities for providing encouragement and infrastructure.

References

[1] M.M.Y. Zaghloul, M.F., Prog. Adhes. Adhes. 34 (2023) 3438
[2] R. Randis, D.B. Darmadi, F. Gapsari, A.A. Sonief, E.D. Akpan, E.E. Ebenso, J. Mol. Liq. 390 (2023) 123067
[3] Issa, T.T., Hasan, J.M., Abdullah, E.T., Shokr, F.S. AIP Conference Proceedings, 2016, 1727, 020012
[4] L.T. Nhiem, D.T.Y. Oanh, N.H. Hieu, Vietnam J. Chem. 61 (2023) 284
[5] S. Kopsidas, G.B. Olowojoba, A.J. Kinloch, A.C. Taylor, Int. J. Adhes. Adhes. 104 (2021) 102723.
[6] E. T. Abdullah, and Omar A. Ibrahim, 62 (2021) 1158
[7] C. Verma, L.O. Olasunkanmi, E.D. Akpan, M.A. Quraishi, O. Dagdag, M. El Gouri, E.M. Sherif, E.E. Ebenso, React. Funct. Polym. 156 (2020) 104741
[8] S. Anwar, X. Li, J. Coat. Technol. Res. 21 (2024) 461
[9] A. Makhmetova, E.S. Negim, D. Ainakulova, G. Yeligbayeva, J. Khatib, Complex Use Miner. Res. Eng. Technol. 328 (2024) 20
[10] M. Samardžija, I. Stojanović, M. Vuković Domanovac, V. Alar, Coatings 13 (2023) 1201
[11 F.H.Mahdi, A.N. Al-Shadeedi, Semiconductors, , 58(2024) 882

[12] B. Su, Y. Zhang, G. Huang, Z. Wang, R. Liu, E3S Web Conf. 213 (2020) 02021
[13] X. Lv, X. Li, N. Li, H. Zhang, Y.Z. Zheng, J. Wu, X. Tao, E3S Web Conf. 2020 (2020) 302021
[14] Maria S. da Dunla, Exp. Theo. NANOTECHNOLOGY 8 (2024) 23
[15] X.-J. Shen, X.-Q. Pei, S.-Y. Fu, K. Friedrich, Polymer 54 (2013) 1234
[16] M. Kim, D.Y. Kim, Y. Kang, O.O. Park, RSC Adv. 5 (2015) 3299
[17] Z.Z. Ali, B.S. Mahdi, A.D. Thamer, Eng. Technol. J. 40 (2022) 1605
[18] E. R, M.H. Moghim, N. Eqra, Polym. Polym. Compos. 29 (2021) S556
[19] M. Naeem, H.C. Kuan, A. Michelmore, S. Yu, A.P. Mouritz, S.S. Chelliah, J. Ma, Carbon 177 (2021) 271
[20] S. Sagadevan, J. Podder, I. Das, J. Mater. Sci. Mater. Electron. 27 (2016) 5622
[21] A. Osman, A. Elhakeem, S. Kaytbay, A. Ahmed, Mater. Chem. Phys. 257 (2021) 123809
[22] X. Wang, X. Qi, Z. Lin, D. Battocchi, Nanomaterials 8 (2018) 1005
[23] J.M. Parente, R. Simões, P.N.B. Reis, Procedia Struct. Integr. 37 (2022) 820
[24] J.S. George, P. Vijayan P, J.K. Paduvilan, N. Salim, J. Sunarso, N. Kalarikkal, N. Hameed, S. Thomas, Prog. Org. Coat. 162 (2022) 106571
[25] Ziyad Khalf Salih, Angham Ayad Kamall-Eldeen, Exp. Theo. NANOTECHNOLOGY 8 (2024) 27
[26] N.I.C. Berhanuddin, I. Zaman, S.A.M. Rozlan, M.A.A. Karim, B. Manshoor, A. Khalid, S.W. Chan, Q. Meng, IOP Conf. Ser.: J. Phys. Conf. Ser. 914 (2017) 012036
[27] Z. A. Hussain and K. A. Saleh, IJP 22 (2024) 90